

Spin Correlations in Actinide Materials: A Neutron Study of USb

G. H. Lander and S. K. Sinha

Argonne National Laboratory, Argonne, Illinois 60439

and

D. M. Sparlin

University of Missouri, Rolla, Missouri 65401

and

O. Vogt

Laboratorium für Festkörperphysik, Eidgenössische Technische Hochschule, Zurich, Switzerland

(Received 19 December 1977)

Measurements have been made of the short-range spin correlations in USb, a metallic compound that orders antiferromagnetically. The system has no transverse fluctuations, and the longitudinal spin correlations are anisotropic, showing stronger interactions within the ferromagnetic sheets than between them. The results of this and other experiments can be understood with simple concepts involving the bonding of 5*f* electrons.

The electronic structure of actinide (5*f*) inter-metallic systems still presents a major puzzle in solid-state physics. In this Letter we suggest that bonding involving *f* electrons plays a major role in determining the magnetic properties of some of these materials. Although compounds of transplutonium elements have not been studied systematically, present evidence suggests that their properties may be understood with models developed for lanthanide (4*f*) systems. The situation is much more difficult for compounds of lighter actinide elements, in which the 5*f* electrons are spatially diffuse and may interact with the actinide 6*d* electrons, as well as with the ligand wave functions. We wish to focus particular attention on the An*X* (An is uranium or neptunium; *X* is N, P, As, Sb, S, Se, or Te) compounds with the simple NaCl crystal structure, since many properties of these are well known.¹ As an introduction we note the following: (1) All materials are metallic and many have large electronic specific heats. (2) The antiferromagnetic pnictides have magnetic structures which are *all* characterized by (001) ferromagnetic sheets that have the spin direction perpendicular to the sheets and that are stacked in various (often complex) arrays. In USb this stacking is a simple alternating + - + - sequence (type I) but in NpP, for example, a 3+, 3- structure is found. (3) A recent study of the magnetic form factor² of USb shows that the magnetization density of the ground-state wave function is oblate in shape, whereas a consideration of the free-ion and crystal-field effects demands a prolate distribution. (4) As we shall see, in USb, the longitudinal spin-correlation lengths

exhibit a large directional anisotropy, which has not been previously observed in a *cubic* system. (5) In addition, the transverse fluctuations are essentially unobservable even at the critical point.³

Uranium antimonide ($a_0 = 6.197 \text{ \AA}$ at 300 K) orders antiferromagnetically at 241 K with the type-I magnetic structure. The same single crystal described in Ref. 2 was used in the present study. The transition at 241 K is second order and the development of the long-range order is shown in Fig. 1, in which we plot reduced magnetization against reduced temperature. The value of $\beta = 0.32 \pm 0.02$ is in good agreement with that expected from three-dimensional Ising systems

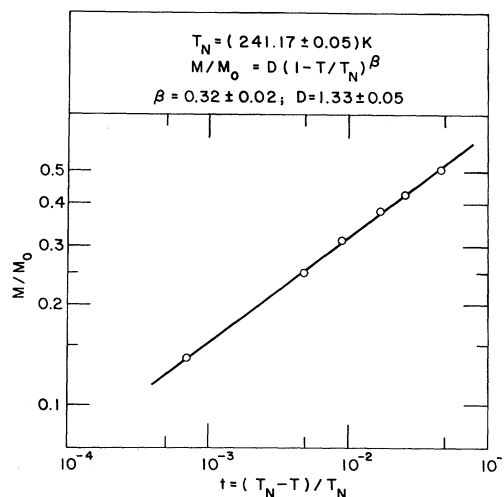


FIG. 1. Reduced magnetization vs reduced temperature below T_N for USb.

($\beta = \frac{5}{18} = 0.3125$). In the ordered state three domains exist in the sample, corresponding to $[100]$, $[010]$, and $[001]$ propagation directions; but the structure factors are such that the scattering at each magnetic zone center arises from a single domain. As in MnF_2 ,⁴ the unique spin direction allows a particularly simple separation of the scattering into transverse and longitudinal components. If the scattering vector, \vec{Q} , is placed parallel to $[001]$ then transverse components only are sampled, whereas with $\vec{Q} \parallel [110]$ both transverse and longitudinal components contribute to the neutron cross section.

The experiments were performed at the CP-5 research reactor with both two- and three-axis neutron spectrometers. The resolution functions were mapped out with the (110) magnetic Bragg reflection and full resolution corrections have been made. With the two-axis instrument an incident neutron beam of wavelength 1 \AA was obtained from the (113) planes of a germanium monochromator. This configuration had less than 0.01% of $\lambda/2$ contamination. To visualize the experimental method we have drawn the $[1\bar{1}0]$ projection of the reciprocal lattice in the upper half of Fig. 2. Bragg points from the fcc atomic structure are (000) and (111) . In principle, both (001) and (110) are magnetic points arising from magnetic domains with a $[001]$ propagation direction. However, no Bragg peak occurs at (001) because the spin direction is then parallel to the scattering vector. Around the (001) point we should observe transverse fluctuations of the spin system in the critical region. The result of a scan from C to C' at $T_N + 3 \text{ K}$ is shown in the lower part of Fig. 2. No critical scattering has been observed around the (001) point, or equivalent (100) and (010) points, at any temperature. Quantitatively we can say that $\chi_T < 0.01\chi_L$, where χ_T is the transverse susceptibility and χ_L , the longitudinal susceptibility. This is an important result, with two immediate consequences: (1) The anisotropy is considerable—one could even argue that it defines an Ising system. (2) The critical scattering at the (110) position represents the longitudinal susceptibility directly.

At the (110) position we can perform scans in two directions. These are shown as AA' and BB' in the upper part of Fig. 2. The actual scans at 244.5 K are shown in the lower part of Fig. 2. [The points in the scan AA' are actually data from a transverse scan through the (011) point because this has the best resolution to define the half-width.] The critical scattering is by no means

isotropic around the (110) point, but shows a very diffuse nature along the direction parallel to the spin direction. Such behavior is very reminiscent of two-dimensional systems, such as K_2NiF_4 ,⁵ in which the scattering near T_N appears in the form of rods of intensity. However, this behavior has not been observed in *cubic* materials. We have also examined the scattering around a number of other Bragg points out of the $(1\bar{1}0)$ plane. From these scans we find that a constant-intensity contour of scattering around a recipro-

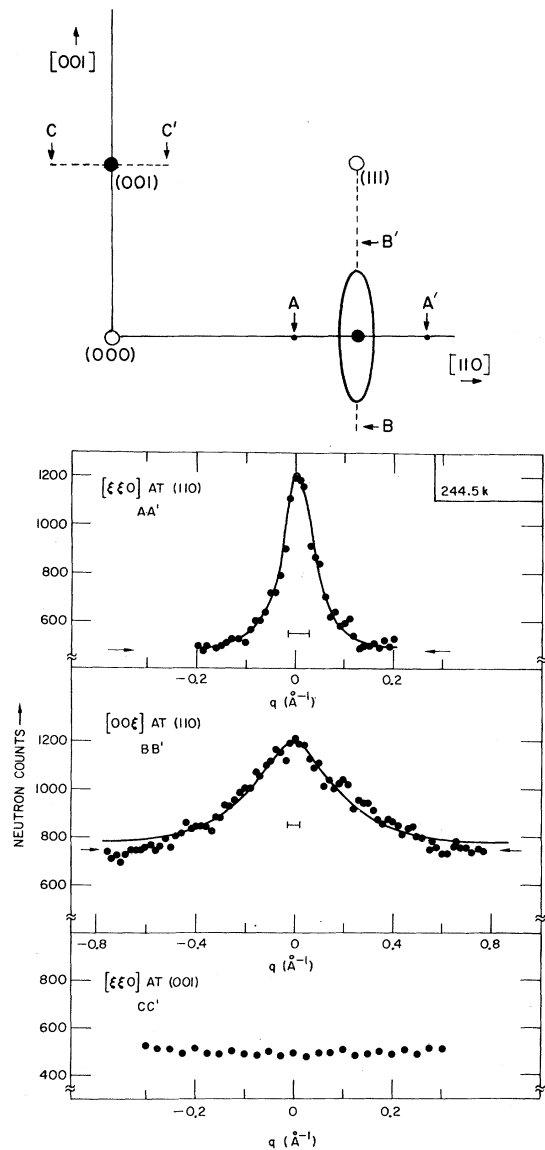


FIG. 2. Upper section, $[1\bar{1}0]$ projection of the reciprocal lattice for USb. Lower section, experimental points and least-squares fits (solid lines) for the scans as shown in the upper section.

cal lattice point may be represented by a cigar with its long axis parallel to the spin direction sampled by that particular domain. The contours perpendicular to the long axis are circular—as required by the tetragonal symmetry of the microscopic fluctuations.

We have also searched for an inelastic component to the critical scattering above T_N with a three-axis spectrometer. We have folded the four-dimensional resolution function with a Lorentzian form for the energy dependence of the cross section,

$$d^2\sigma/d\Omega d\omega \propto \chi_L(q, T)\Gamma/(\Gamma^2 + \omega^2), \quad (1)$$

where q is the reduced wave vector measured from the (110) point, T the temperature, and Γ a characteristic frequency. We conclude that the longitudinal fluctuations exhibit *no* observable inelasticity, $\Gamma < 0.05$ THz. This implies that the fluctuations are long lived, $> 2 \times 10^{-11}$ sec at all temperatures, and that the two-axis data can be used without any corrections.

We now turn to the analysis of the longitudinal fluctuations. The simplest assumption is that the Ornstein-Zernicke form is followed; then the cross section, integrated over energy and generalized to include anisotropic interaction, may be written

$$\frac{d\sigma}{d\Omega} = A(T)f^2(\vec{Q}) \left[\kappa_{\parallel}^2 + q_{\parallel}^2 + \left(\frac{\kappa_{\parallel}}{\kappa_{\perp}} \right)^2 q_{\perp}^2 \right]^{-1}, \quad (2)$$

where $A(T)$ is a slowly varying function of T , $f(\vec{Q})$ is the form factor, which is a constant over the range of $|\vec{Q}|$ sampled in this experiment, and κ_{\perp} and κ_{\parallel} are the inverse correlation ranges of the *longitudinal fluctuations* perpendicular and parallel to the unique spin direction, respectively. The procedure is then to fold this cross section with the resolution function and least-squares fit to the experimental data. The fits to the data are reasonable (Fig. 2), except that scans such as BB' indicate that the assumption of a Lorentzian may be too simple, and that the quantitative values of κ_{\parallel} should be treated with some caution. Nevertheless, values for κ_{\parallel} from the two-axis and three-axis instruments are in good agreement, despite the very different configurations used. From Fig. 3 we can make the following observations: (1) The ratio of the major to minor axes of the "cigar" of critical scattering is independent of temperature, and from a least-squares fit $\kappa_{\parallel}/\kappa_{\perp} = 5.0 \pm 0.5$. (2) The exponential decay of the inverse correlation length follows the power

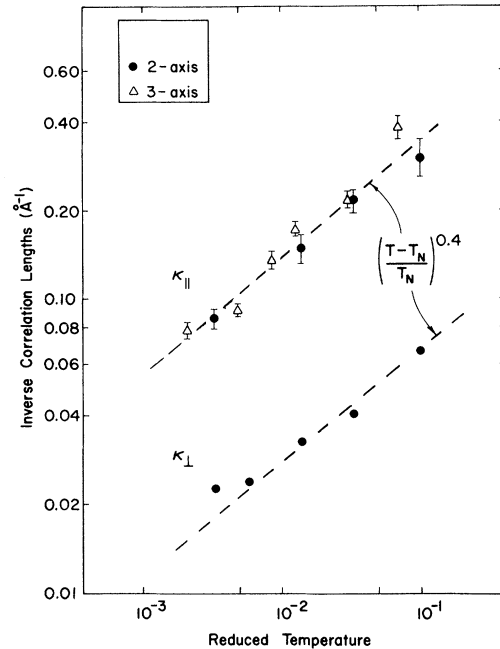


FIG. 3. Inverse correlation lengths for the longitudinal fluctuations for USb as a function of reduced temperature. Thus κ_{\perp} comes from analyzing scans such as AA' in Fig. 2, and κ_{\parallel} from BB' . (The error bars for κ_{\perp} are the size of the points.)

law $\kappa \propto [(T - T_N)/T_N]^{0.40 \pm 0.05}$. This exponent ν in the theory of critical phenomena has the values 0.5 for mean field theory, 0.643 for a 3D (three-dimensional) Ising system, and 1 for a 2D Ising system. Our value is below the theoretical expectations; however, before evaluating the significance of ν (and by implication γ and η) derived here, we must be certain that we are within the critical regime. Considerable uncertainty surrounds this point in the present experiment. The absolute value of κ_{\parallel} ranges from 0.08 to 0.35 \AA^{-1} over the reduced temperature examined. In real space, therefore, κ_{\parallel}^{-1} is between 12 and 3 \AA which is very small. On the other hand, the interaction between the sheets is almost certainly of the Ruderman-Kittel-Kasuya-Yosida type, which is long range, and the complex stacking arrangements found in similar systems¹ suggests that the range R of the interaction is as long as three or four unit cells, $R \sim 15 \text{\AA}$. Hence $\kappa_{\parallel}R > 1$, whereas the scaling hypotheses that govern the derivation of critical exponents require $\kappa R \ll 1$.

All experimental evidence to date suggests that these systems are Ising-like, with the spins locked normal to the (001) sheets and strongly coupled within the sheets. We believe that these

properties are a consequence of strong hybridization of the $5f$ orbitals on the uranium atom with neighboring anion p orbitals and possibly also with nearest-neighbor uranium d orbitals to form the bonding states. A consideration of the geometry of the NaCl structure and the f , p , and d orbitals shows that the energy gained from the in-plane 2D bonding arrangement in the oblate configuration (relative to $[001]$) is greater than that gained from bonding arrangements normal to the plane in the prolate configuration, because of the smaller number of bonding orbitals in the latter case. If this "bonding" energy is greater than the crystal-field energy, this would explain why the ground state of the uranium atom is different from that expected from crystal-field considerations, as revealed by the form factor measurements,² and also the Ising-like nature. The bonding picture also explains why the correlations between the spins on the uranium ions within the (001) sheets are strong, since this interaction is transmitted via the direct overlap of neighboring orbitals, whereas the interaction between the sheets must rely on the weaker indirect conduction-electron-exchange mechanism. We thus have a system in which the magnetic ordering is not dominated completely either by indirect exchange between localized moments (as in the $4f$ series) or by an interaction primarily between spins of itinerant electrons (as in the $3d$ metals),

but in which the bonding involving $5f$ electrons coupled with the strong spin-orbit interaction plays an important role in the development of long-range magnetic order. Further experimental and theoretical investigations of these intriguing systems are in progress.

We are grateful to R. L. Hitterman for experimental assistance. This work was supported by the U. S. Department of Energy.

¹A. T. Aldred and D. J. Lam, in *The Actinides: Electronic Structure and Related Properties*, edited by A. J. Freeman and J. B. Darby (Academic, New York, 1974), Vol. I, Chap. 3.

²G. H. Lander, M. H. Mueller, D. M. Sparlin, and O. Vogt, *Phys. Rev. B* **14**, 5035 (1976).

³G. H. Lander, D. M. Sparlin, and O. Vogt, in *Magnetism and Magnetic Materials—1976*, AIP Conference Proceedings No. 34, edited by J. J. Becker and G. H. Lander (American Institute of Physics, New York, 1976). Similar anomalies have been found in measurements on UN; see W. J. L. Buyers, T. M. Holden, E. C. Svensson, and G. H. Lander, in Proceedings of the International Conference on Neutron Inelastic Scattering, Vienna, October 1977 (International Atomic Energy Agency, to be published).

⁴M. P. Schulhof, P. Heller, R. Nathans, and A. Linz, *Phys. Rev. B* **1**, 2304 (1970).

⁵R. J. Birgeneau, J. Skalyo, and G. Shirane, *Phys. Rev. B* **3**, 1736 (1971), and *J. Appl. Phys.* **41**, 1303 (1970).

Spatial Condensation of Strain-Confined Excitons and Excitonic Molecules into an Electron-Hole Liquid in Silicon

P. L. Gourley and J. P. Wolfe

University of Illinois at Urbana-Champaign, Urbana, Illinois 61801

(Received 14 November 1977)

By direct spatial imaging and spectral analysis of recombination luminescence we have observed in silicon (1) the drift of photoproduced excitons from the crystal surface into a strain potential well; (2) ideal-gas behavior of the strain-confined excitons in the well between 25 and 5 K; (3) a real-space condensation near $T = 4$ K which defines the first-order gas-liquid phase transition; and (4) luminescence from excitonic molecules.

In this Letter we report observations of luminescence from free excitons (FE), excitonic molecules (EM), and electron-hole liquid (EHL) confined within a strain-induced potential well inside a pure Si crystal. Above $T = 5$ K the FE luminescence exhibits a Gaussian spatial profile $\exp(-\alpha x^2/kT)$ expected for an ideal gas in a parabolic potential well, $V = \alpha r^2$. Near 4 K the spatial profile abruptly narrows and luminescence from

the liquid phase appears, indicative of a first-order phase transition. By this means we have produced for the first time in Si a large volume of EHL with greatly enhanced lifetime. We report the first images of these excitonic phases in Si.

An appealing aspect of the strain-confinement technique is that it produces a well-defined spatial distribution of excitons in the semiconductor.